ELSEVIER

Contents lists available at ScienceDirect

# Journal of Theoretical Biology

journal homepage: www.elsevier.com/locate/yjtbi





## Emergent trade-offs among plasticity strategies in mixotrophs

Kevin M. Archibald a,\*, Stephanie Dutkiewicz b,c, Charlotte Laufkötter d,e, Holly V. Moeller a

- <sup>a</sup> Department of Ecology, Evolution, and Marine Biology, University of California Santa Barbara, Santa Barbara, CA, USA
- b Department of Earth, Atmospheric, and Planetary Sciences, Massachusetts Institute of Technology, Cambridge, MA, USA
- <sup>c</sup> Center for Global Change Science, Massachusetts Institute of Technology, Cambridge, MA, USA
- <sup>d</sup> Climate and Environmental Physics, University of Bern, Bern, Switzerland
- <sup>e</sup> Oeschger Centre for Climate Change Research, University of Bern, Bern, Switzerland

## ARTICLE INFO

#### Keywords: Mixotrophy Metabolic plasticity Food web model

## ABSTRACT

Marine mixotrophs combine phagotrophy and phototrophy to acquire the resources they need for growth. Metabolic plasticity, the ability for individuals to dynamically alter their relative investment between different metabolic processes, allows mixotrophs to efficiently exploit variable environmental conditions. Different mixotrophs may vary in how quickly they respond to environmental stimuli, with slow-responding mixotrophs exhibiting a significant lag between a change in the environment and the resulting change metabolic strategy. In this study, we develop a model of mixotroph metabolic strategy and explore how the rate of the plastic response affects the seasonality, competitive fitness, and biogeochemical role of mixotroph populations. Fastresponding mixotrophs are characterized by more efficient resource use and higher average growth rates than slow-responding mixotrophs because any lag in the plastic response following a change in environmental conditions creates a mismatch between the mixotroph's metabolic requirements and their resource acquisition. However, this mismatch also results in increased storage of unused resources that support growth under future nutrient-limited conditions. As a result of this trade-off, mixotroph biomass and productivity are maximized at intermediate plastic response rates. Furthermore, the trade-off represents a mechanism for coexistence between fast-responding and slow-responding mixotrophs. In mixed communities, fast-responding mixotrophs are numerically dominant, but slow-responding mixotrophs persist at low abundance due to the provisioning effect that emerges as a result of their less efficient resource acquisition strategy. In addition to increased competitive ability, fast-responding mixotrophs are, on average, more autotrophic than slow-responding mixotrophs. Notably, these trade-offs associated with mixotroph response rate arise without including an explicit physiological cost associated with plasticity, a conclusion that may provide insight into evolutionary constraints of metabolic plasticity in mixotrophic organisms. When an explicit cost is added to the model, it alters the competitive relationships between fast- and slow-responding mixotrophs. Faster plastic response rates are favored by lower physiological costs as well as higher amplitude seasonal cycles.

## 1. Introduction

Mixotrophs, organisms that acquire the resources needed for growth through both autotrophic and heterotrophic metabolic processes, are widespread among marine microbial communities (Hartmann et al., 2012; Flynn et al., 2013; Leles et al., 2017; Stoecker et al., 2017). While mixotrophy broadly classifies a wide array of behaviors and nutritional modes, here we focus on the combination of phagotrophy and phototrophy commonly found in planktonic protists (Jones, 1997; Mitra et al., 2016). Specifically, we consider constitutive mixotrophs (those with an inherent capacity for photosynthesis) grazing on bacterial prey (Stoecker et al., 2017). The metabolic flexibility achieved through mixotrophy provides a number of evolutionary benefits that,

as evidenced by the ubiquity of these organisms, appear to provide advantages outweighing the increased physiological cost of maintaining two sets of metabolic machinery (Ward et al., 2011; Selosse et al., 2017). In highly seasonal environments, for example, mixotrophs can adapt their metabolic strategy to follow large changes in environmental conditions (Li et al., 2000; Litchman, 2007). Mixotrophs are also common in low-seasonality, oligotrophic environments where phagotrophy helps to supplement the nutrient demands of photosynthetic plankton (Havskum and Hansen, 1997; Zubkov and Tarran, 2008).

Many mixotrophs display significant metabolic plasticity — the ability to alter their relative investment into different metabolic processes in response to environmental conditions (Lie et al., 2018; Wilken et al.,

E-mail address: karchibald@ucsb.edu (K.M. Archibald).

Corresponding author.

2020). The emergence of specific mixotrophic strategies along gradients of environmental resources (e.g. light, nutrients, prey) has been described using both experimental and modeling approaches (Fischer et al., 2017; Edwards, 2019; Schenone et al., 2022). These relationships create a dynamic balance between phagotrophy and phototrophy that varies as a function of environmental conditions (Adolf et al., 2006; Flynn and Mitra, 2009; Schenone et al., 2022) and results in the succession of different strategies throughout seasonal cycles (Berge et al., 2017). This metabolic plasticity has both ecological and biogeochemical relevance since it can affect net community production, the transfer of biomass to higher trophic levels, and the efficiency of the biological pump (Mitra et al., 2013; Ward and Follows, 2016).

Does the flexibility provided by plasticity come at a cost to the organism? Mixotrophs that combine phagotrophy and phototrophy are typically less efficient at resource acquisition and may have lower growth rates compared to specialists (Litchman et al., 2007; Pérez et al., 1997; Zubkov and Tarran, 2008). These trade-offs may be explained by fundamental physiological constraints based on cell surface area and volume when mixotrophs partition space between different metabolic strategies (Litchman et al., 2007; Ward et al., 2011). More broadly, the idea that phenotypic plasticity is associated with some fundamental cost to the organism's fitness is often cited as an explanation for why species are not infinitely plastic (DeWitt et al., 1998; Murren et al., 2015). In empirical studies, however, estimates of the magnitude of the negative fitness effects of plasticity are often quite small (e.g. see meta-analysis by Van Buskirk and Steiner (2009)).

Furthermore, the question of whether phenotypic plasticity has a positive or negative effect on interspecies competition remains unclear (Turcotte and Levine, 2016). Several studies have found that plasticity promotes coexistence by reducing the strength of competitive interactions through increased niche partitioning (Nilsson, 1967; Lepik et al., 2005; Ashton et al., 2010; Eloranta et al., 2011; Lipowsky et al., 2015). Other studies have found that plasticity impedes coexistence (Aerts et al., 1991; Bret-Harte et al., 2001) and increases invasion success (Molina-Montenegro et al., 2012), or has no effect on competitive ability (Milberg et al., 2014).

Plasticity is often discussed in terms of the range of phenotypes that an individual exhibits (i.e. more plastic individuals have a wider range of possible phenotypes). Plastic responses, however, have a significant time component as well. For mixotrophs, the timescale of plastic responses is potentially non-trivial considering the significant reallocation of resources within the cell required to alter the nutritional mode when multiple types of metabolic machinery are involved. If the time required to execute that reallocation results in a significant lag following a shift in environmental conditions, there may be a period of time during which the mixotroph is performing sub-optimally while it transitions towards some theoretically defined optimal strategy. Here, we describe different plastic mixotrophs in terms of the time scale of their response to environmental variability; fast-responding mixotrophs are able to alter their metabolic strategy quickly in response to changing environmental conditions while slow-responding mixotrophs experience significant lag between an environmental stimulus and their plastic response. Our primary aim is to understand how the timescale of a mixotroph's plastic response affects its ecological and biogeochemical characteristics.

In this study, we extend the model framework developed by Klausmeier et al. (2004b,a) to represent the variable allocation strategies in a constitutive mixotroph grazing on heterotrophic bacteria in a seasonal environment. Our model simulates the dynamics of two essential resources, carbon and nitrogen, in a simple food chain consisting of a mixotroph and its bacterial prey. This simplified trophic structure was identified as an essential step in describing the fundamental mechanisms associated with the time scale of mixotroph plastic response before incorporating these behaviors into more complex food web models. In our model, we do not assign a nutritional strategy *a priori*, but instead allow a growth-maximizing strategy to emerge as a function

of environmental conditions (Klausmeier et al., 2004b,a; Berge et al., 2017) that mixotroph populations converge to at a rate determined by their plastic response rate. We use this model in three different sets of experiments to explore the following questions: (1) How does the rate of the plastic response affect the seasonality of mixotroph metabolic strategy? (2) What is the optimal (i.e. most competitive) plasticity under different assumptions of cost and seasonal amplitude? And (3) What trade-off mechanisms allow for coexistence between mixotroph populations with different plasticity?

We use this model to show how trade-offs between mixotrophs with different plasticity strategies emerge from ecologically mediated environmental feedbacks. Mixotrophs with faster plastic response rates benefit from higher average growth rates and those with slower response rates benefit from increased resource provisioning. As a result, intermediate plasticity strategies maximize mixotroph biomass and productivity, as well as provide a mechanism for coexistence between populations with differing degrees of plasticity. Notably, these trade-offs arise from simple growth maximization principles and without any explicit physiological cost to plasticity, thereby providing an alternative hypothesis for constraints on the evolution of increased metabolic plasticity in marine mixotrophs.

#### 2. The mixotroph model

The model (Fig. 1) follows a population of mixotrophs growing in a well-mixed water column under periodic environmental forcing (Fig. 2a–c) due to changes in mixed layer depth (H, which affects inorganic nutrient supply), temperature (T), and light intensity at the surface ( $I_0$ ). The mixotroph population is represented by cell abundance (M) and the per-cell internal quotas of carbon ( $Q_C$ ) and nitrogen ( $Q_N$ ). Carbon is acquired by mixotrophs from two sources: photosynthesis and the consumption of heterotrophic bacteria (B). The functional response for each process assumes Michaelis–Menten dynamics (Michaelis and Menten, 1913). Internal carbon quotas are consumed during mixotroph growth, where the specific mixotroph growth rate ( $\mu$ ) is a function of  $Q_C$  and  $Q_N$ . The rate of change of  $Q_C$  is then given by,

$$\frac{dQ_C}{dt} = \frac{v_I I}{k_I + I} + \frac{b_C v_G B}{k_G + B} - \mu(Q_C, Q_N) Q_C, \tag{1}$$

with maximum photosynthetic rate  $v_I$ , photosynthetic half-saturation constant  $k_I$ , maximum grazing rate  $v_G$ , grazing half-saturation constant  $k_G$ , and bacteria per-cell carbon content  $b_C$ . Light is attenuated over the water column with exponential coefficient  $k_d$ , so the average light intensity experienced by mixotrophs in the mixed layer (I) depends on both the intensity at the surface and the depth of the water column following,

$$I = \frac{I_0}{k_d H} (1 - e^{-k_d H}). \tag{2}$$

Similarly, nitrogen is acquired via uptake of inorganic nitrogen from the environment (N) and from grazing on bacteria:

$$\frac{dQ_N}{dt} = \frac{v_N N}{k_N + N} + \frac{b_N v_G B}{k_G + B} - \mu(Q_C, Q_N) Q_N, \tag{3}$$

with maximum nutrient uptake rate  $v_N$ , nutrient uptake half-saturation constant  $k_N$ , and bacteria per-cell nitrogen content  $b_N$ . We assume that mixotroph growth is limited by either carbon or nitrogen and calculate growth rate using a minimization function following Droop's model (Droop, 1968),

$$\mu(Q_C,Q_N) = \mu_{max} min \left[ 1 - \frac{Q_{min,C}}{Q_C}, 1 - \frac{Q_{min,N}}{Q_N} \right], \tag{4} \label{eq:power_def}$$

where  $\mu_{max}$  is the theoretical maximum growth rate under infinite quota conditions and  $Q_{min,C}$  and  $Q_{min,N}$  are the minimum required quotas of carbon and nitrogen, respectively. Mixotroph biomass increases as a result of growth and decreases through two mortality terms: a linear mortality rate (a) and an additional term  $(s^+)$  that represents dilution

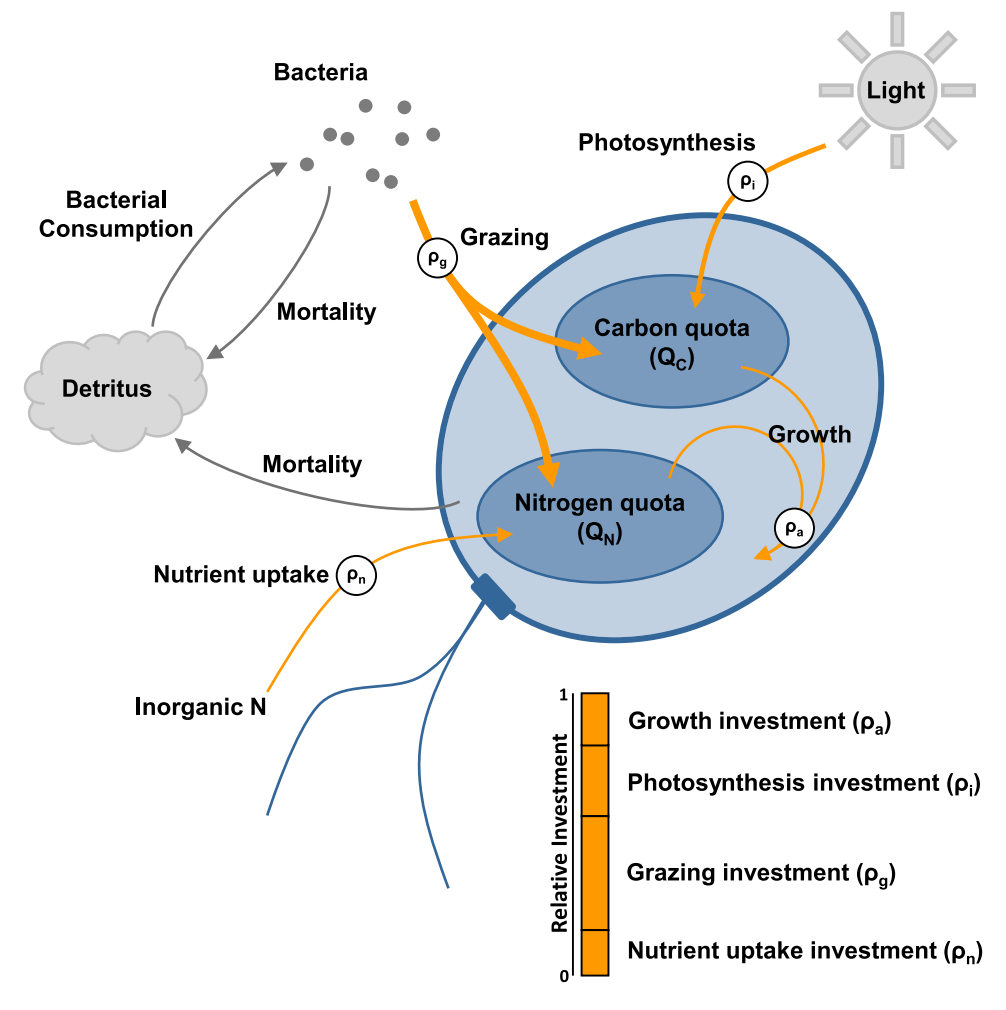


Fig. 1. Model of mixotroph metabolism. A population of mixotroph cells is characterized by the per-cell internal reserves, or quotas, of carbon  $(Q_C)$  and nitrogen  $(Q_N)$ . Photosynthesis and grazing on bacteria supply carbon to the mixotroph. Grazing also supplies nitrogen alongside the uptake of inorganic nitrogen from the environment. Mixotrophs consume their internal C- and N-quotas to fuel population growth. Mortality supports a pool of detritus that serves as food for the bacteria population. Metabolic strategies are plastic and vary based on the mixotroph's relative investment into each metabolic process, represented by the  $\rho$  values:  $\rho_i$  represents investment into photosynthesis,  $\rho_g$  investment into growth.

due to the entrainment of deep water when the mixed layer depth is increasing,

$$\frac{dM}{dt} = \mu(Q_C, Q_N)M - aM - s^+M. \tag{5}$$

Dilution depends on the rate of change of the mixed layer depth, dH/dt, and is inversely proportional to the current mixed layer depth (Freilich et al., 2021). Concentrations do not change when the mixed layer depth is decreasing (shoaling), so dilution is equal to zero under these oceanographic conditions.

$$s^{+} = \begin{cases} \frac{1}{H} \frac{dH}{dt} & \text{if } \frac{dH}{dt} > 0\\ 0 & \text{if } \frac{dH}{dt} \le 0. \end{cases}$$
 (6)

Mixotroph mortality, as well as mortality in the bacteria population, contributes to a pool of detritus (D), which we choose to track in terms of nitrogen content. This simplification follows from the assumption that bacteria are always nitrogen limited and obtain their nitrogen solely from the uptake of detritus. Because detrital uptake determines bacterial production, any carbon implicitly contained in the detrital pool in excess to the bacterial C:N ratio is lost. The rate of change of D is given by,

$$\frac{dD}{dt} = a(b_n B + Q_N M) - \frac{v_B D b_N B}{k_B + D} - s^+ D, \tag{7}$$

where  $v_B$  and  $k_B$  are the uptake rate and half-saturation constant of D by bacteria, respectively. A portion (r) of the detritus consumed by the bacteria is remineralized into inorganic nutrients such that,

$$\frac{dN}{dt} = s^{+}(N_0 - N) - \frac{v_N M N}{kn + N} + \frac{r v_B D b_N B}{k_B + D},$$
(8)

where  $N_0$  is the nutrient concentration below the mixed layer. The remainder of the detritus taken up by the bacteria is assimilated into biomass

$$\frac{dB}{dt} = \frac{(1-r)v_B DB}{k_B + D} - \frac{v_G BM}{k_G + B} - aB - s^+ B. \tag{9}$$

Temperature scaling

Seasonal variability in temperature affects several biological rates in the model including growth ( $\mu_{max}$ ), photosynthesis ( $v_I$ ), nutrient uptake ( $v_N$ ), grazing ( $v_G$ ), and bacterial production ( $v_B$ ). Temperature-sensitive parameters are represented as exponentially increasing functions of temperature relative to a known rate at reference temperature  $T_0$ ,

$$x = x_0 Q_{10}^{(T - T_0)/10}. (10)$$

All temperature-sensitive parameters in the model were assigned the same  $Q_{10}$  coefficient of 1.88 following Eppley (1972). It should

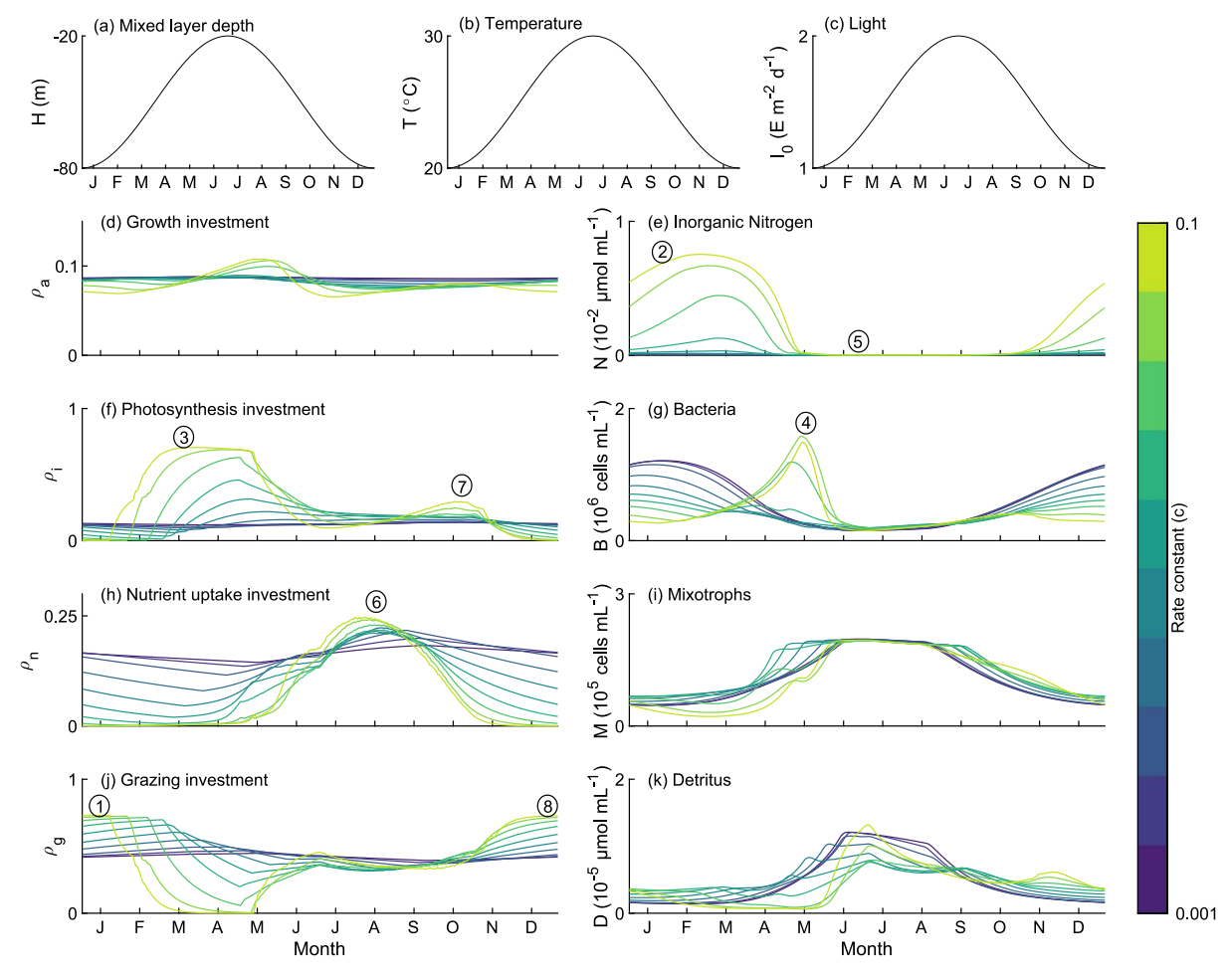


**Fig. 2.** Population experiment: Dependence of ecosystem seasonal dynamics on the plasticity rate constant (c). Seasonal drivers, mixed layer depth (a), temperature (b), and light (c) are shown in the top row. The mixotroph investment strategies (d,f,h,j) impact, and are in turn impacted by, temporal dynamics in resource availability and biomass (e,g,i,k). Times series are shown for different values of the plasticity constant c and represent the final year of a ten-year simulation, with numbered annotations to show key features. Over winter, light is at a minimum and the availability of inorganic nitrogen is high due to deep mixing. To meet their carbon requirements, mixotrophs increase grazing investment (1) and decrease photosynthesis and nitrogen uptake investment. Reduced nitrogen uptake by mixotrophs supplements deep mixing and contributes to high nitrogen availability during the winter (2). In spring, rising light levels and high inorganic nitrogen concentrations make photosynthetic niches more optimal and mixotrophs respond by increasing investments into photosynthesis (3), while simultaneously decreasing investments into grazing. During this period of largely autotrophic growth, bacteria populations reach a maximum (4). By summer, the water column has become highly stratified and nitrogen concentrations are significantly reduced (5). Now strongly nitrogen-limited, mixotrophs invest primarily into inorganic nutrient uptake (6) with a combination of both photosynthesis and grazing to meet their carbon needs. During fall, light decreases and vertical mixing increases inorganic nitrogen concentration. The fast-responding mixotrophs display a short-lived burst of photosynthetic investment during this period (7) before light levels fall low enough that photosynthesis is an inefficient source of carbon. As light levels continue to decline into the winter, mixotrophs once again increase their investment into grazing (8).

be noted that several theoretical and empirical arguments have been made that heterotrophic metabolic processes may be more sensitive to temperature than autotrophic processes (López-Urrutia et al., 2006; Rose and Caron, 2007) and that these differences in sensitivity amplify the thermal responses of marine food webs (Archibald et al., 2022), but here we use a standardized  $Q_{10}$  for all biological rates as a useful simplification. Mixotrophs, in their capacity to combine phagotrophy and phototrophy, may be uniquely influenced by variability across thermal sensitivity coefficients (Gonzalez et al., 2022). While assuming a standardized  $Q_{10}$  is useful for simplifying our analysis in the current study, relaxing this assumption to explore the effects of variable thermal sensitivity would add valuable future context to the results presented here.

### Metabolic investments

Mixotroph metabolic strategy is represented by the population's investment into photosynthesis, grazing, the uptake of inorganic nutrients, and a generalized growth term that represents cell division. For simplicity, we assume that the cellular structures associated with each of these metabolic processes have the same elemental stoichiometry

to eliminate any variability in nutrient requirements as a function of investment, although mixotroph stoichiometry has been shown to vary significantly based on prey composition (Chrzanowski et al., 2010) and may help to stabilize environmental element ratios (Moorthi et al., 2017). We implement metabolic investments by scaling the following model parameters by an associated investment factor ( $\rho$ ) following the analysis in Klausmeier et al. (2004a),

$$\mu_{max} = \rho_a \mu'_{max} \tag{11}$$

$$v_I = \rho_i v_I' \tag{12}$$

$$v_N = \rho_n v_N' \tag{13}$$

$$v_G = \rho_g v_G'. \tag{14}$$

The trade-off between investing in different metabolic processes is represented by an additional constraint, such that,

$$\rho_a + \rho_i + \rho_n + \rho_g = p, (15)$$

where p is the proportion of mixotroph biomass committed to metabolism. The metabolic strategy of the mixotroph population

Table 1
Variables and parameter values used in the simulation of the mixotroph model

| Symbol              | Description                                | Value                                  | Units                               |  |
|---------------------|--|--|-------------------------------------|--|
| Н                   | Mixed-layer depth                          |  | m                                   |  |
| Т                   | Temperature                                |  | °C                                  |  |
| $I_0$               | Light intensity at surface                 | $E m^{-2} day^{-1}$                    |                                     |  |
| I                   | Average light intensity over mixed layer   |  | E m <sup>-2</sup> day <sup>-1</sup> |  |
| N                   | Inorganic nitrogen                         |  | $\mu$ mol N mL $^{-1}$              |  |
| В                   | Bacterial abundance                        |  | cells mL <sup>-1</sup>              |  |
| D                   | Detritus                                   |  | μmol N mL <sup>-1</sup>             |  |
| M                   | Mixotroph abundance                        | cells mL <sup>-1</sup>                 |                                     |  |
| N                   | Inorganic nitrogen                         | $\mu$ mol N mL <sup>-1</sup>           |                                     |  |
| $Q_{C}$             | Mixotroph carbon quota                     | μmol C cell <sup>-1</sup>              |                                     |  |
| $Q_N$               | Mixotroph nitrogen quota                   | μmol N cell <sup>-1</sup>              |                                     |  |
| $o_a$               | Investment in growth                       |  | •                                   |  |
| $o_i$               | Investment in photosynthesis               |  |                                     |  |
| $o_n$               | Investment in nitrogen uptake              |  |                                     |  |
| $\rho_g$            | Investment in grazing                      |  |                                     |  |
| 2                   | Plasticity rate constant                   | [10 <sup>-3</sup> , 10 <sup>-1</sup> ] | day <sup>-1</sup>                   |  |
| ε                   | Cost of plasticity                         | [0, 100]                               | •                                   |  |
| $u_b$               | Bacteria growth rate                       | 1.0                                    | day <sup>-1</sup>                   |  |
| a                   | Mortality rate                             | 0.05                                   | day <sup>-1</sup>                   |  |
| u'                  | Maximum mixotroph growth rate              | 5.4                                    | day-1                               |  |
| <br>g'              | Maximum grazing rate                       | 4.0                                    | day <sup>-1</sup>                   |  |
| $v'_i$              | Maximum photosynthetic rate                | $3.33 \times 10^{-7}$                  | μmol C cell <sup>-1</sup> day       |  |
|                     | Maximum grazing rate                       | 4.0                                    | day <sup>-1</sup>                   |  |
| $v_g'$ $v_n'$       | Maximum nitrogen uptake rate               | $1.36 \times 10^{-6}$                  | μmol N cell <sup>-1</sup> day       |  |
| k <sub>i</sub>      | Light half-saturation constant             | 5                                      | E m <sup>-2</sup> day <sub>-1</sub> |  |
| $k_n$               | Nitrogen half-saturation constant          | $5.6 \times 10^{-3}$                   | μmol N mL <sup>-1</sup>             |  |
|                     | Grazing half-saturation constant           | $8 \times 10^{5}$                      | cells mL <sup>-1</sup>              |  |
| k <sub>g</sub>      | Bacterial growth half-saturation constant  | $1 \times 10^{-5}$                     | μmol N mL <sup>-1</sup>             |  |
| k <sub>b</sub><br>r | Remineralization fraction                  | 0.3                                    | μιιοι iv iiiL                       |  |
|                     | Light attenuation coefficient              | 0.05                                   | $m^{-1}$                            |  |
| k <sub>d</sub>      | Metabolic cell fraction                    | 0.03                                   | 111                                 |  |
| p<br>b              | Carbon content of bacteria                 | $1.67 \times 10^{-8}$                  | μmol C cell <sup>-1</sup>           |  |
| b <sub>C</sub>      | Carbon content of assembly machinery       | $350.9 \times 10^{-9}$                 | μmol C                              |  |
| $C_a$               | · · ·                                      | $350.9 \times 10^{-9}$                 | μmol C                              |  |
| $C_i$               | Carbon content of photosynthetic machinery |  |                                     |  |
| $C_n$               | Carbon content of uptake machinery         | $350.9 \times 10^{-9}$                 | μmol C                              |  |
| $C_g$               | Carbon content of grazing machinery        | $350.9 \times 10^{-9}$                 | μmol C                              |  |
| C <sub>o</sub>      | Carbon content of non-metabolic biomass    | $350.9 \times 10^{-9}$                 | μmol C                              |  |
| $b_N$               | Nitrogen content of bacteria               | $3.14 \times 10^{-9}$                  | μmol N cell <sup>-1</sup>           |  |
| $N_a$               | Carbon content of assembly machinery       | $45.4 \times 10^{-9}$                  | μmol N                              |  |
| $N_i$               | Carbon content of photosynthetic machinery | $45.4 \times 10^{-9}$                  | μmol N                              |  |
| $N_n$               | Carbon content of uptake machinery         | $45.4 \times 10^{-9}$                  | μmol N                              |  |
| $N_g$               | Carbon content of grazing machinery        | $45.4 \times 10^{-9}$                  | μmol N                              |  |
| $N_o$               | Carbon content of non-metabolic biomass    | $45.4 \times 10^{-9}$                  | μmol N                              |  |
| $T_0$               | Thermal scaling reference temperature      | 20                                     | °C                                  |  |
| $Q_{10}$            | Thermal scaling coefficient                | 1.88                                   |                                     |  |

**Table 2**Summary of experiments conducted including number of mixotroph types in each simulation, the parameter(s) varied over repeated simulations in the experiment, and the intended purpose of the experiment.

| Experiment | Mixotroph types | Parameter varied                       | Purpose                                |
|------------|-----------------|--|--|
| Population | 1               | Rate constant (c)                      | Ecological and biogeochemical dynamics |
| Community  | 10              | Cost $(\epsilon)$ , seasonal amplitude | Effects of cost, optimal plasticity    |
| Pairwise   | 2               |  | Mechanisms of coexistence              |

changes through time following,

$$\frac{d\rho}{dt} = (\hat{\rho} - \rho)c,\tag{16}$$

where  $\hat{\rho}$  is the growth-optimizing strategy for the current environmental conditions and c is a rate constant describing the time scale of the plastic response. As the model is simulated forward through time, the metabolic strategy that maximizes growth at any given time (defined below) changes as a function of temperature, light, nutrient concentration, and bacterial abundance. The mixotroph population changes its current investment strategy to follow this moving target. The time scale over which it responds to changes in the environment depends on the parameter, c. Mixotrophs that can respond quickly to changing environmental conditions, and are capable of making large jumps through metabolic phase space, are assigned large values of c and represent "fast-responding" mixotrophs. Mixotrophs that respond

more slowly to environmental change have small values of  $\boldsymbol{c}$  and are characterized as "slow-responding".

The determination of the instantaneous growth-optimizing metabolic strategy is a maximization problem of the function  $\mu(Q_C,Q_N)$  over  $\rho$ . We assume that the internal cell quotas equilibrate quickly relative to the time scale of environmental variance and solve for the quasi-equilibrium by setting  $\frac{dQ}{dt}=0$ .

$$\tilde{Q}_C = Q_{min,C} + \frac{1}{\mu_{max}} \left( \frac{v_I I}{k_I + I} + \frac{b_C v_G B}{k_G + B} \right) \tag{17}$$

$$\tilde{Q}_N = Q_{min,N} + \frac{1}{\mu_{max}} \left( \frac{v_N N}{k_N + N} + \frac{b_N v_G B}{k_G + B} \right)$$
(18)

The growth rate of the mixotroph is determined by the minimum limiting resource (carbon or nitrogen) and is equal to the minimum of the C-limited and N-limited growth rates. A full expression for the

growth rate as a function of  $\rho$  can be found by substituting Eqs. (11)–(14) into (17)–(18) and substituting the resulting expressions for  $\tilde{Q}_C$  and  $\tilde{Q}_N$  into (4).

$$\mu(\rho_{1}, \rho_{2}, \rho_{3}, \rho_{4}) = \min \left[ \frac{\rho_{1} \mu'_{max} \frac{\rho_{2} v'_{1} I}{k_{I} + I} + \frac{\rho_{4} v'_{G} b_{C} B}{k_{G} + B}}{\rho_{1} \mu'_{max} Q_{min,C} + \frac{\rho_{2} v'_{1} I}{k_{I} + I} + \frac{\rho_{4} v'_{G} b_{C} B}{k_{G} + B}}, \dots \right]$$

$$\frac{\rho_{1} \mu'_{max} \frac{\rho_{3} v'_{N} N}{k_{N} + N} + \frac{\rho_{4} v'_{G} b_{N} B}{k_{G} + B}}{\rho_{1} \mu'_{max} Q_{min,N} + \frac{\rho_{3} v'_{N} N}{k_{N} + N} + \frac{\rho_{4} v'_{G} b_{N} B}{k_{G} + B}}$$
(19)

We used the MATLAB function *fminimax* (Optimization Toolbox: Version 9.0, R2020b) to numerically estimate the values of  $\rho$  that maximize (19) for a given set of environmental conditions (I, N, B, T). The resulting  $\rho$  values represent the growth-optimizing metabolic strategy ( $\hat{\rho}$ ). The additional constraint in (16) is applied during this optimization to ensure that  $\hat{\rho}$  has unit sum and that (16) is conserved through the dynamic evolution of the mixotroph's metabolic strategy.

#### Costs of plasticity

Metabolic plasticity may come at a cost to the organism (Pérez et al., 1997; Litchman et al., 2007; Zubkov and Tarran, 2008). In order to change its metabolic strategy a mixotroph must commit energy and resources to building new cellular machinery and dismantling the old. We introduce a cost function (*Y*) that scales the population growth rate proportionally to the magnitude of the total change in metabolic investment,

$$Y = e^{-\epsilon \sum_{i=1}^{4} \frac{d\rho_i}{dt}}.$$
 (20)

The cost function Y multiplies the mixotroph growth rate such that growth is reduced under higher plasticity costs. Substituting (20) into (4), we update the expression for mixotroph growth such that,

$$\mu(Q_C, Q_N) = Y \mu_{max} min \left[ 1 - \frac{Q_{min,C}}{Q_C}, 1 - \frac{Q_{min,N}}{Q_N} \right], \tag{21}$$

The parameter  $\epsilon$  is the relative cost of plasticity. Y is defined such that if the mixotroph's metabolic strategy is stable (e.g., constant environmental conditions) the cost is zero. Negative effects on growth rate are only realized when the mixotroph is actively changing its metabolic investments and scales with the magnitude of those changes. Other implementations of cost functions, such as a cost to plasticity that is constant in time, are possible, but this realized cost approach was selected as the most relevant to our model setup that includes time-variable investments.

## Numerical integration

The parameters values used in the simulation of the model are summarized in Table 1. We ran three sets of experiments (Table 2). First, we ran a population experiment composed of repeated, independent model runs over a range of c. The model setup included a single mixotroph with a different c value per simulation. All simulations had the same cost of plasticity,  $\epsilon = 0$ . The model was spun up for 10 years, with the final year used for analysis. Next, we ran a community experiment using a model setup that included 10 different mixotrophs with various c values competing against each other. Repeated model runs were conducted, changing the cost of plasticity ( $\epsilon$ ) and the amplitude of the seasonal cycle each time. Finally, we ran a pairwise competition experiment consisting of a single simulation using a model that included just two mixotrophs types with different c values. The dynamics in this pairwise experiment were simpler than the community experiment and were helpful in describing specific coexistence mechanisms between a fast-responding and a slow-responding mixotroph.

We tested several initial conditions, and found that running our model for 10 years allowed transient dynamics from initial conditions to disappear and that different simulations converged on the same results (Supplementary Fig. S1). In the case of low-plasticity mixotrophs (small c), we initialized the metabolic strategies using the emergent optimal strategies of the highest-plasticity mixotrophs (large c) to limit the transient behavior to a few annual cycles and reduce computational time. Integration of the mixotroph model is limited by the computationally expensive maximization problem used to determine the growth-optimizing metabolic strategy at each time point. To reduce simulation time, we introduce a new variable,  $\omega$ , that describes the frequency that the optimal strategy is calculated. During the integration, the optimal strategy is calculated at regular time intervals every  $1/\omega$  units. The sensitivity of our results to  $\omega$  is shown in Supplemental Figure S2.

## 3. Model analysis

Population experiment: Intermediate plasticity maximizes productivity

First, we examine the output of the population experiment, composed of independently simulated model runs that each include a single mixotroph and use a different c value per simulation. The experiment shows how seasonal dynamics depend on the plasticity rate constant. Both fast- and slow-responding mixotroph types showed similar seasonal patterns in metabolic strategy, although fast-responding mixotrophs had larger amplitude changes in investment and more metabolic variability over the year (Fig. 2). Variability in metabolic strategy over the seasonal cycle has several significant feedbacks onto the ecosystem. Reduced investment into inorganic nitrogen uptake during the winter, for example, amplifies the already high wintertime nitrogen concentrations. During the spring bloom, when mixotrophs become more autotrophic, bacteria populations are released from grazing and increase in abundance, supporting increased nutrient recycling. The increased plasticity observed in mixotrophs with higher c values (i.e. greater range of metabolic strategies) strengthens these feedbacks and magnify the mixotroph's biogeochemical impact on ecosystem function.

Interestingly, fast-responding mixotrophs do not have higher peak abundances than slow-responding mixotrophs (Fig. 2i). While fastresponding mixotrophs have optimized their metabolic strategy to maximize their growth rate for the current conditions, there is an emergent trade-off to this strategy due to ecological feedbacks in the system. Consider the differences in metabolic strategy between fast- and slowresponding mixotrophs during the winter (Fig. 2, left column). During this time period, mixotroph growth is limited by carbon due to the combination of low light and high inorganic nitrogen concentration (Fig. 3). The instantaneous growth-maximizing strategy under these conditions is to become more heterotrophic since grazing is a more efficient source of carbon than photosynthesis under low light conditions. Fast-responding mixotrophs react quickly to these constraints and drastically increase their investment into grazing, while simultaneously decreasing their investments into both photosynthesis and nutrient uptake. Slow-responding mixotrophs experience similar incentives to become more heterotrophic and move in the same direction (in trait space) as fast-responding mixotrophs. However, their slower response is characterized by lower grazing rates and higher nutrient uptake rates over the winter. Although these slow-responding mixotrophs achieve lower growth rates in the short term because of the mismatch between their nutrient requirements and their metabolic strategy, the tempered response has two important consequences. First, the reduced grazing pressure allows bacteria populations to remain higher over the winter months, sustaining a critical carbon supply and higher rates of remineralization. Second, the higher uptake of inorganic nitrogen at a time period when it is not limiting means that slow-responding mixotrophs build up large reserves of nitrogen over the winter (Fig. 3).

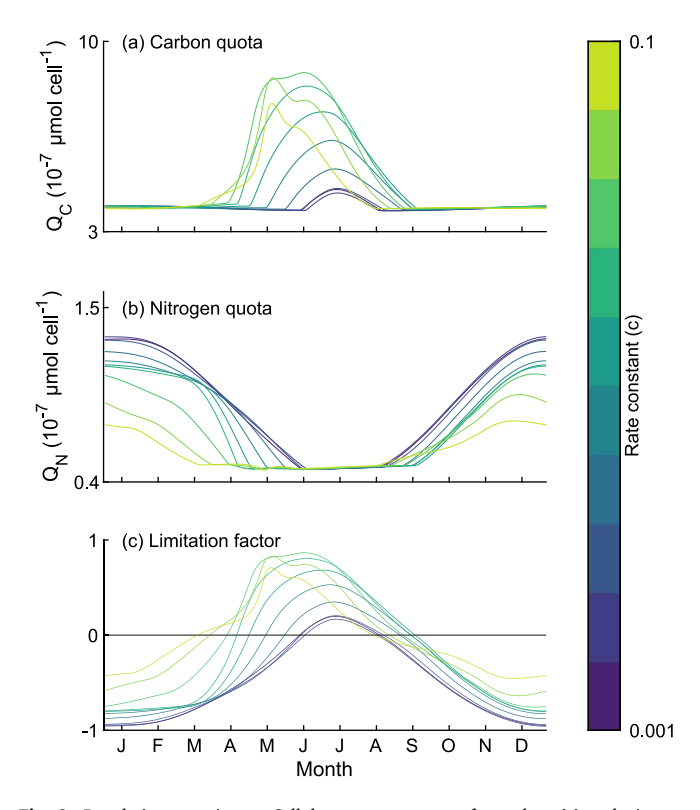


Fig. 3. Population experiment: Cellular resource quotas for carbon (a) and nitrogen (b) and the resulting resource limitation factor (c) over the seasonal cycle for various values of the plasticity rate constant (c). Limitation factors are calculated as  $log_{10}\left(\frac{Q_c}{Q_{max}}/\frac{Q_{max}}{Q_{minx}}\right)$ . A positive value indicates N-limitation and a negative value indicates C-limitation. Across all population simulations, mixotrophs are N-limited in the summer and C-limited in the winter. Slow-responding mixotrophs accumulate greater reserves of nitrogen during the winter, which supports springtime growth and results in the transition to N-limitation significantly later in the season.

By spring, when the water column begins to stratify, these reserves of nitrogen ensure that slow-responding mixotrophs do not become nitrogen-limited until much later in the seasonal cycle, compared to their fast-responding counterparts (Fig. 3).

The longer time scale of the plastic response in slow-responding mixotrophs "accidentally" creates resource reserves that support higher productivity rates in the early spring, as well as earlier initiation of the spring bloom and earlier peak abundance (Fig. 2). We say accidentally because this positive effect is not accounted for by the growth-maximization function and emerges as a secondary effect due to slow-responding mixotrophs less plastic response. The slow-responding mixotroph becomes trapped within a narrow area of the trait space because the time scale of seasonal change is shorter than the time scale of the plastic response. The instantaneous growth-maximizing strategy represents a moving target that each mixotroph is chasing and slow-responding mixotrophs alter their strategy too slowly to ever make it far from the average strategy. The end result is that the slowresponding mixotroph adopts a more stable metabolic strategy suited for the average conditions they experience, which provides emergent benefits in the form of resource provisioning.

Because rapid response rates have both positive (growth rate maximization) and negative (over-grazing and reduced resource provisioning) effects on mixotroph populations, productivity and seasonally integrated biomass are both maximized at an intermediate plasticity level that balances the pros and cons of metabolic variability (Fig. 4). The unimodal shape of the relationship reflects the trade-off between adaptation to environmental variability and a more tempered strategy that maintains metabolic diversity and buffers mixotrophs against large seasonal shifts with increased resource storage. We use "trade-off" even

though the mixotrophs are not choosing between the costs and benefits of rapid plastic responses.

The trade-off between fast-responding mixotrophs that make large changes to their metabolic strategy season to season and slow-responding mixotrophs that maintain a more consistent strategy also affects the biogeochemical role of mixotroph populations. Highly plastic mixotrophs become more autotrophic during the spring and more heterotrophic during the winter (Fig. 2). In contrast, less plastic mixotrophs maintain more balanced levels of heterotrophy and autotrophy throughout the season. As a result, the fast-responding mixotrophs create greater variability in their carbon balance, becoming a carbon sink in the spring and carbon source in the winter. Because the productivity signal tends to be dominated by the highly productive spring growing season, fast-responding mixotrophs are, on average, more autotrophic than slow-responding mixotrophs (Fig. 4).

## Community experiment: Optimal plasticity balances costs and benefits

While intermediate plasticity mixotrophs have the highest productivity, that does not necessarily make those types the most competitive. Next, we examine the output of the community experiment to understand how differing plasticity rate constants affect competitive ability. This experiment is composed of multiple model runs that each include a community of 10 mixotroph types with various plasticity rates (c). Repeated runs were conducted using different costs for plasticity ( $\epsilon$ ) and different amplitudes of the seasonal cycle. In model runs where  $\epsilon = 0$ , the numerically dominant mixotroph in the simulated community is the fastest-responding mixotroph (highest c value; Fig. 5a). For higher values of  $\epsilon$ , this competitive advantage is offset by a higher physiological cost to plasticity. As the cost increases, the community is dominated by mixotrophs with intermediate c values (Fig. 5b). If the cost is sufficiently high, the numerically dominant mixotroph type becomes the mixotroph with the smallest c value (Fig. 5c). Additionally, coexistence between fast- and slow-responding mixotroph types is observed at all cost levels (including  $\epsilon = 0$ ). Here, we define coexistence as persistence over long time scales (at least 20 years).

The optimal rate constant, defined as the value of c assigned to the numerically dominant mixotroph type, is inversely related to the cost of plasticity (Fig. 6). This relationship is further modulated by the amplitude of the seasonal cycle. Large amplitude seasonal cycles create more environmental variability and therefore larger potential benefits of plasticity. Environments with large amplitude seasonal cycles more strongly select for higher plasticity than low-amplitude environments (Fig. 6).

Pairwise experiment: Nutrient provisioning allows slow-responding mixotrophs to persist

Community-scale simulations of the model show that coexistence is possible between fast- and slow-responding mixotrophs (Fig. 5). Next, we turn to the output of the pairwise experiment to examine in more detail the mechanisms that allow a slow-responding mixotroph to persist with a more competitive, fast-responding mixotroph. This experiment consists of a single model run using two mixotroph types with different c values. The c values used in this simulation are the maximum (c=0.1) and minimum (c=0.001) of the range this parameter across all experiments in order to maximize the competitive difference between the mixotroph types.

The same trade-offs that result in slow-responding mixotrophs achieving higher productivity allow these mixotrophs to persist when competing against fast-responding competitors. A mixotroph type with a higher c value will generally have higher growth rate because it can more quickly reach the growth-maximizing metabolic strategy for any give set of environmental conditions. In a competitive scenario, the benefits of a stable strategy that a slow-responding mixotroph adopts are reduced, since resources that would have been "saved" for

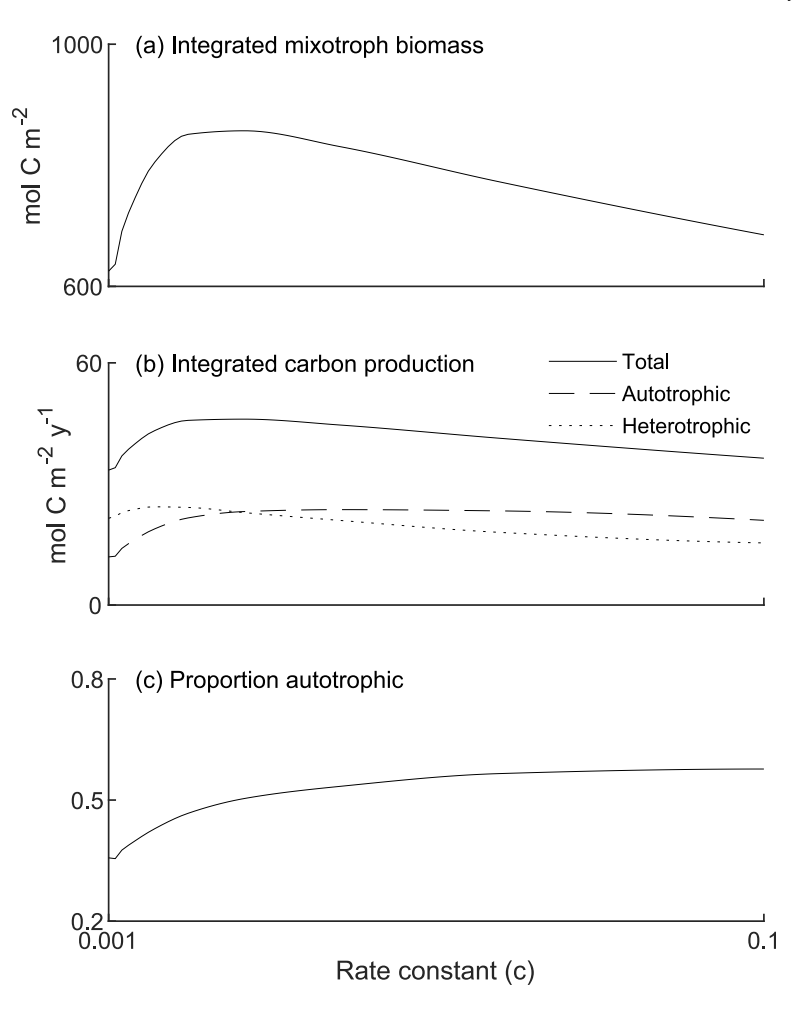


Fig. 4. Population experiment: Annually integrated mixotroph biomass (a), mixotroph C-production (b) and the proportion of C-production from autotrophic metabolism (c) as a function of the plasticity rate constant (c). Both biomass and productivity are maximized for intermediate values of c as a result of emergent trade-offs between fast- and slow-responding strategies.

future growth are instead consumed by the competitor. Nevertheless, in the pairwise experiment, the slow-responding mixotroph is able to persist due to higher growth rates in the late spring fueled by accumulated nitrogen reserves. Slow-responding mixotrophs maintain a higher investment in nutrient uptake during the carbon-limited winter months and generate excess nitrogen reserves that they can draw from in the spring when the water column stratifies. The resulting delay in becoming nitrogen limited creates a narrow window during the spring when slow-responding mixotrophs can outgrow fast-responding mixotrophs (Fig. 7), thus persisting against a more plastic competitor.

#### 4. Discussion

In this study, we extend existing models of plankton physiology (Klausmeier et al., 2004b,a) to develop a new framework to represent mixotroph metabolic plasticity within a simple food chain. This new model does not assign a specific metabolic strategy but allows optimal investments to emerge based on growth rate maximization principles. We use the model to simulate seasonal dynamics in mixotroph strategy for various rates of plastic responses and explore how this time scale affects the ecological characteristics and biogeochemical consequences of mixotroph populations. The model reveals a trade-off between fast-responding and slow-responding mixotrophs that allows the persistence of less competitive, slow-responding mixotrophs due to an emergent resource provisioning effect. Interestingly, this effect arises incidentally from the mixotroph's slower response time to environmental change and requires no foresight or planning on behalf of the individual.

Furthermore, the trade-off emerges without any explicit physiological cost to plasticity and may help explain the apparent constraints to the evolution of increased plasticity (DeWitt et al., 1998; Murren et al., 2015).

### Plasticity and time scale

One unique feature of our modeling framework is the inclusion of an explicit time scale in the plastic response. We define a strategy that maximizes growth rate based on current conditions and allow mixotrophs to asymptotically converge towards this theoretical optimum at a prescribed rate. This definition distinguishes our model from previous models that typically focus on the optimality criteria themselves (e.g. growth optimization, competitive outcomes) (Klausmeier et al., 2004b,a; Edwards, 2019). The inclusion of transient states as mixotrophs dynamically adapt to variable environmental conditions provides a new dimension to modeling metabolic plasticity. Furthermore, this approach reduces the model's dependence on initial assumptions because the range of phenotypes exhibited by a mixotroph emerges as a function of environmental variability and the rate of the plastic response, rather than being assigned a priori.

This framework also adds memory to the model. That is, a mixotroph's time-evolving metabolic strategy depends on past conditions as well as current conditions because a mixotroph must move from a previous state to a new state by crossing the intervening trait space. In a periodic environment, such as a seasonal cycle, a memory property connects our representation of plastic changes back to the

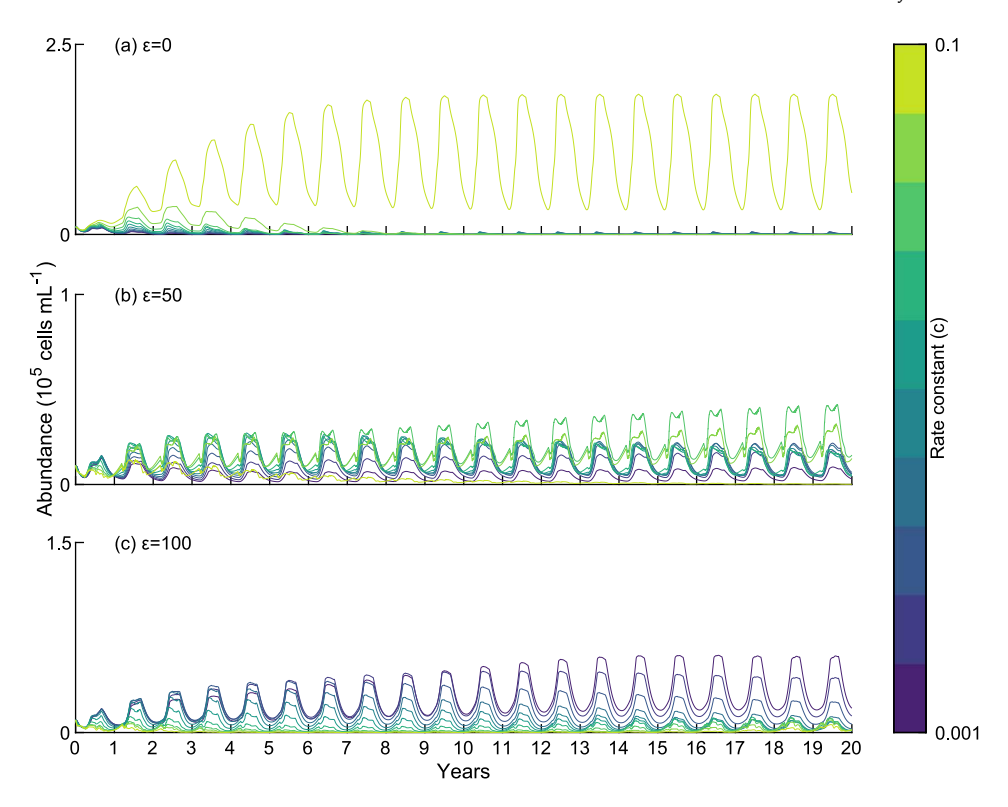


Fig. 5. Community experiment: Time series of community simulations for three different values of cost  $(\epsilon)$  showing the abundance of each mixotroph type. Communities are numerically dominated by fast-responding mixotrophs when the cost is low and become dominated by increasingly more slow-responding mixotrophs as  $\epsilon$  increases. Coexistence between types is possible at all cost levels, though the abundance of slow-responding mixotrophs may be very low for small values of  $\epsilon$ .

traditional dogma that defines plasticity as the range of traits that an individual can exhibit. A slow-responding mixotroph exhibits only a narrow range of metabolic strategies over a seasonal cycle because its longer response restricts its metabolic mobility; by the time it responds to an environmental change and moves in one direction, the environment has shifted back in the opposite direction and the mixotroph must reverse course. In contrast, fast-responding mixotrophs can quickly make large changes and exhibit a much broader range of strategies at different points in the seasonal cycle.

## Trade-offs emerge without explicit physiological costs

Metabolic plasticity has a number of clear benefits: it allows for more efficient growth under variable food conditions (Auer et al., 2015), stabilizes population dynamics (Bolker et al., 2003; Miner et al., 2005), and increases resilience to environmental change (Seebacher et al., 2015). Given these benefits, it is generally assumed that plasticity must be limited by fundamental physiological constraints, or cost (DeWitt et al., 1998; Beaman et al., 2016). We offer an alternative explanation for the evolution of low-plasticity mixotrophs, however, by detailing the emergence of a trade-off that is entirely independent of any physiological cost: When low-plasticity (i.e. slow-responding) mixotrophs lag behind the growth-maximizing strategy, they create a mismatch between their resource uptake and nutrient requirements that results in the accumulation of nitrogen during time periods when carbon is limiting. These excess nitrogen reserves come at the cost of lower growth efficiency in the moment, but provide an advantage under future stratified conditions. While this post hoc benefit is not accounted for in the mixotroph's response to environmental variability, nevertheless, the implicit trade-off it creates results in mixotroph biomass and productivity reaching their maximum value at intermediate plasticity values that achieve some balance between the advantages of high- and low-plasticity strategies.

This emergent trade-off bears similarity to the concept of "bethedging", a term that describes various traits or strategies that decrease temporal fitness variation at the cost of reduced average, or expected, fitness (reviewed by Seger et al. (1987)). Bet-hedging has been described in many different contexts, including the maintenance of genetic polymorphism (Christiansen, 1974; Walsh, 1984), species coexistence in variable environments (Warner and Chesson, 1985), and the evolution of reproductive strategies (Kaplan and Cooper, 1984). By adopting a trait or strategy that may reduce their fitness now, organisms can buffer themselves against large swings in fitness when conditions change. Low-plasticity mixotrophs in variable environments benefit from maintaining a diversified metabolic strategy that reflects the average conditions rather than the immediate conditions. Reduced variability in their strategy results in excess uptake and storage of currently unneeded resources that provide reserves during nutrientlimited conditions in the future, thereby reducing variability in their fitness over the course of the seasonal cycle at the cost of a lower average growth rate. In our model, while bet-hedging is not an explicit strategy, something like bet-hedging arises due to the slow response time of less plastic mixotrophs. The emergence of these benefits suggest that such bet-hedging behaviors could actually arise evolutionarily from selection upon variability in plastic response rates. Bethedging may provide other long-term advantages as well, such as reducing mixotrophs' dependence on any single resource and increasing resilience to environmental variability (Stoecker, 1998).

Other theoretical frameworks, including fitness sets (Levins, 1962), may be valuable in interpreting the evolutionary context for temporal variability in mixotroph metabolic strategy as well. A fitness set is a way of graphically depicting the optimality of different phenotypes in variable environments by plotting the trade-off curve of combinations of phenotypes alongside contours of constant fitness (Levins, 1962). Under this framework, overall fitness is reduced by environmental variance while phenotypic plasticity serves to restore a portion of this fitness loss, albeit never to the level that would be achieved in

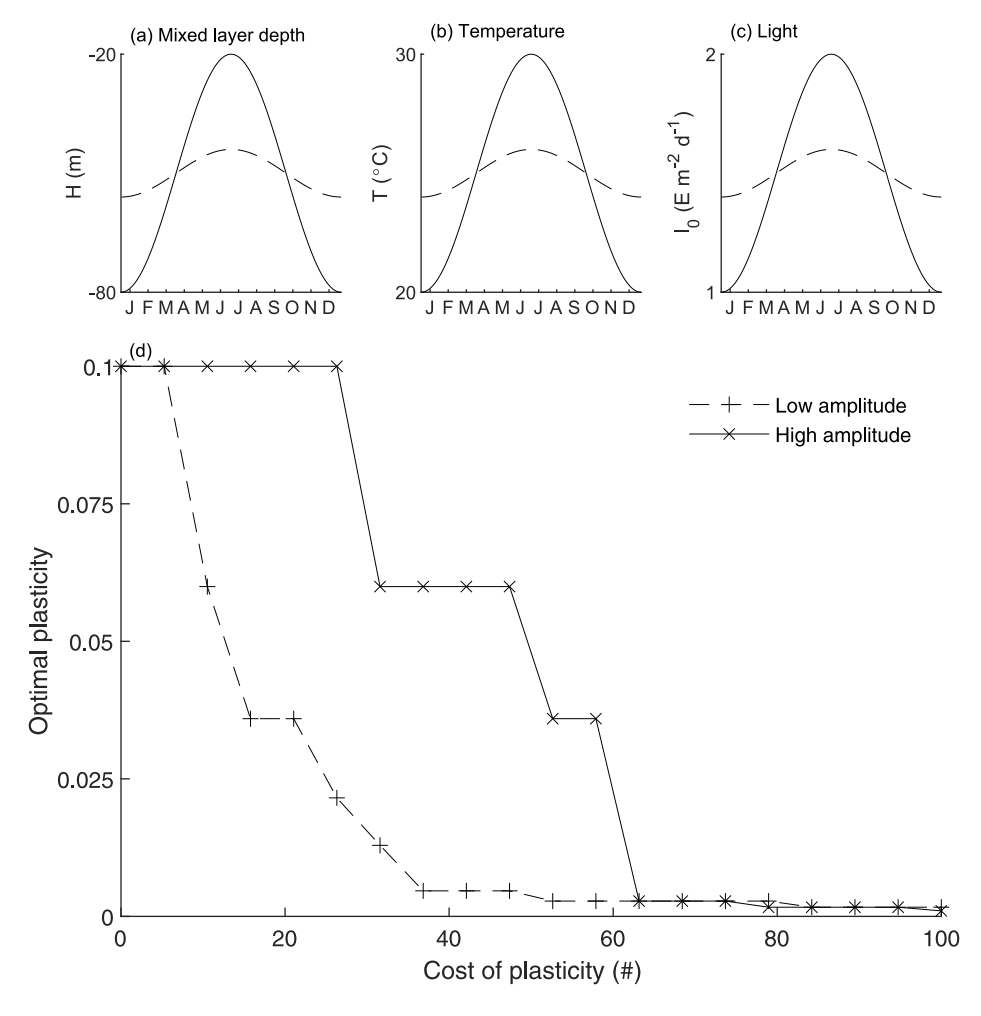


Fig. 6. Community experiment: Optimal rate constant (c) as a function of the cost of plasticity ( $\epsilon$ ) for two different environments. Low and high amplitude environments are defined by the annual range of three drivers: mixed layer depth (a), temperature (b), and light (c). The optimal rate constant (d) is defined as the value of c of the mixotroph type that is numerically dominant in a community. Optimal rate constants decline as the cost increases, with higher amplitude seasonal cycles favoring higher values of c. Crosses indicate simulation points.

a constant environment (Levins, 1968). Our model predicts a similar relationship, with higher plasticity in more variable environments (Fig. 6). An in-depth analysis of fitness set theory and its ecological and evolutionary applications can be found in Levins (1968).

## Biogeochemical implications

One unique aspect of studying metabolic plasticity in mixotrophs is the combination of both autotrophic and heterotrophic processes within the same organism. Variable investment into phototrophy versus phagotrophy has the potential to create shifts in the carbon sourcesink dynamics of marine plankton communities. Where mixotrophs contribute significantly to overall production and respiration, plastic changes to metabolic strategy may act like a fulcrum in calculations of net community production (NCP), shifting the ecosystem between states of net autotrophy and net heterotrophy on sub-seasonal time scales. This balance represents a critical component of the carbon cycle since marine food webs account for approximately half of global primary productivity (Field et al., 1998) and export about 10 Pg C y<sup>-1</sup> into the deep ocean via the biological pump (Nowicki et al., 2022). Simulations of our model showed that fast-responding mixotrophs are more autotrophic, thereby contributing to increased NCP, although this conclusion is contingent on significant seasonality of the system and different relationships may emerge in other biogeochemical regimes. Although direct measurements of seasonal variability in mixotrophic metabolic strategies in situ are lacking, the simulated seasonality in our

model is consistent with general expectations that mixotrophic strategies are more common during stratified summer months in temperate ecosystems, while autotrophic strategies are more common during the spring bloom (e.g., Berge et al. (2017), Edwards (2019) and Millette et al. (2021)).

One important caveat to the observed biogeochemical consequences in this study is the limited trophic resolution of our model, which includes only mixotrophs and their bacterial prey without either specialized autotrophs (phytoplankton) or specialized heterotrophs (zooplankton). The simplified model structure was chosen to isolate interactions between mixotroph metabolism and the environment. Our model excludes several important ecosystem carbon fluxes, including phytoplankton-zooplankton grazing dynamics, that likely play an important role in modulating mixotroph metabolic strategies alongside the mixotroph-environment feedbacks described in this study. For example, previous modeling work has also shown that competition can drive trait displacement; mixotrophs occupy a more heterotrophic niche when competing with phytoplankton, for example (Chu et al., 2023). Future models that resolve these interactions will help constrain the ecosystem-level biogeochemical role of mixotroph plasticity. Furthermore, the flexibility provided by food web models (compared to linear food chains) may buffer the model against sensitivity to structural changes and perform better at capturing important seasonal behaviors (Pahl-Wostl, 1997; Fulton et al., 2003), although very complex models often suffer from parameter uncertainty due to their tendency to propagate error (Iwasa et al., 1987).

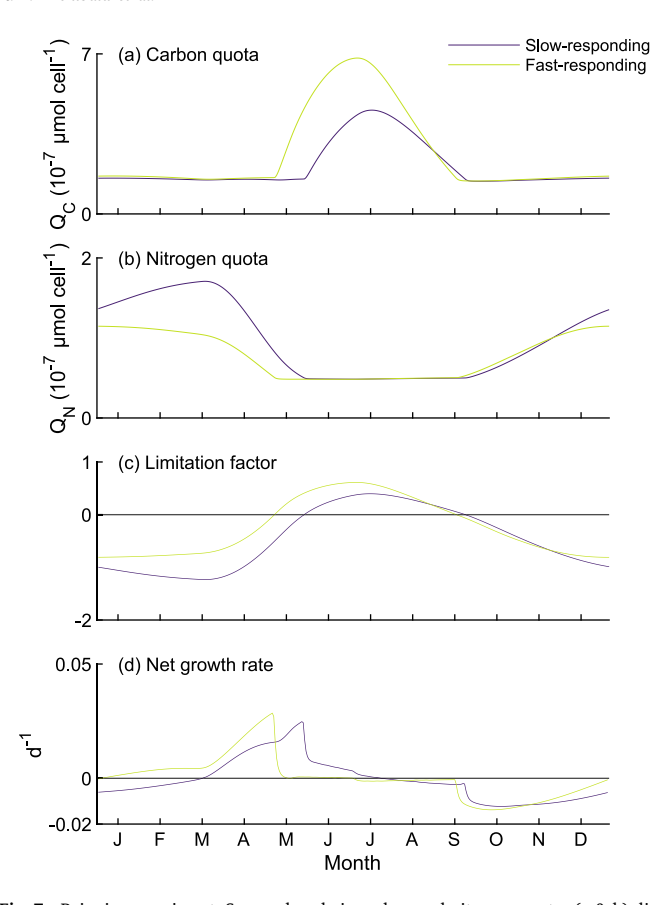


Fig. 7. Pairwise experiment: Seasonal cycle in carbon and nitrogen quotas (a & b), limitation factor (c), and net growth rates (d) for fast- (green) and slow-responding (blue) mixotrophs in a pairwise competition experiment. The slow-responding mixotroph is able to persist due to a period in late spring during which its growth rate is higher than that of the fast-responding mixotroph because of large nitrogen reserves accumulated during the winter months. These nitrogen reserves help mitigate N-limitation during in May and June when the water column is stratifying.

We have also excluded energetic considerations when constructing the model in favor of simplicity. Energetic growth efficiency is generally lower in autotrophic compared to heterotrophic microbes, with mixotrophs falling somewhere in the middle (Yang et al., 2000; Li et al., 2020). This physiological cost of autotrophy is absent from the model's metabolic optimization algorithm, which assumes perfect growth efficiency for both heterotrophic and autotrophic processes in the growth maximization calculation (19). Such a cost may constrain investments into photosynthesis and moderate the tendency for more plastic mixotrophs to be, on average, more autotrophic.

## Model applications

A shifting paradigm in recent years has emphasized the importance of mixotrophy in marine microbial food webs (Flynn et al., 2013; Stoecker et al., 2017). Our results highlight complex ecological dynamics arising from variance in mixotroph metabolic strategy that may have significant evolutionary implications for existing patterns of variation in mixotroph plasticity. Although logistically challenging, future experimental studies that quantify mixotroph plasticity in situ could test the mechanisms described by the model and give insight into standing mixotroph phenotypic variation and its implications for biogeochemical cycling. Complimenting empirical measurements, our model also provides a framework that could be incorporated into spatially explicit food web models to better understand the mechanisms that drive spatial and temporal variability in mixotroph metabolic strategy at a global scale.

#### CRediT authorship contribution statement

Kevin M. Archibald: Methodology, Formal analysis, Conceptualization, Visualization, Writing – original draft, Writing – review & editing. Stephanie Dutkiewicz: Conceptualization, Methodology, Writing – review & editing. Charlotte Laufkötter: Conceptualization, Methodology, Writing – review & editing. Holly V. Moeller: Conceptualization, Methodology, Writing – review & editing.

## Declaration of competing interest

None.

#### Acknowledgments

Work was supported by the Simons Foundation, USA (990798, K.M.A.; 689265, H.V.M.) and the US National Science Foundation (OCE-1851194, H.V.M.). S.D. is grateful for support from the Simons Collaboration on Computational Biogeochemical Modeling of Marine Ecosystems, USA (CBIOMES; Simons Foundation, 549931) and from NASA, USA (80NSSC23K1232). C.L. acknowledges support from the Swiss National Science Foundation, Switzerland (174124).

## Appendix A. Supplementary data

Supplementary material related to this article can be found online at https://doi.org/10.1016/j.jtbi.2024.111854.

#### References

Adolf, J.E., Stoecker, D.K., Harding, Jr., L.W., 2006. The balance of autotrophy and heterotrophy during mixotrophic growth of karlodinium micrum (dinophyceae). J. Plankton Res. 28 (8), 737–751.

Aerts, R., Boot, R., Van der Aart, P., 1991. The relation between above-and belowground biomass allocation patterns and competitive ability. Oecologia 87, 551-559.

Archibald, K.M., Dutkiewicz, S., Laufkötter, C., Moeller, H.V., 2022. Thermal responses in global marine planktonic food webs are mediated by temperature effects on metabolism. J. Geophys. Res.: Oceans 127 (12), e2022JC018932.

Ashton, I.W., Miller, A.E., Bowman, W.D., Suding, K.N., 2010. Niche complementarity due to plasticity in resource use: plant partitioning of chemical N forms. Ecology 91 (11), 3252–3260.

Auer, S.K., Salin, K., Rudolf, A.M., Anderson, G.J., Metcalfe, N.B., 2015. Flexibility in metabolic rate confers a growth advantage under changing food availability. J. Anim. Ecol. 84 (5), 1405–1411.

Beaman, J.E., White, C.R., Seebacher, F., 2016. Evolution of plasticity: mechanistic link between development and reversible acclimation. Trends Ecol. Evol. 31 (3), 237–249

Berge, T., Chakraborty, S., Hansen, P.J., Andersen, K.H., 2017. Modeling succession of key resource-harvesting traits of mixotrophic plankton. ISME J. 11 (1), 212–223.

Bolker, B., Holyoak, M., Křivan, V., Rowe, L., Schmitz, O., 2003. Connecting theoretical and empirical studies of trait-mediated interactions. Ecology 84 (5), 1101–1114.

Bret-Harte, M.S., Shaver, G.R., Zoerner, J.P., Johnstone, J.F., Wagner, J.L., Chavez, A.S., Gunkelman Iv, R.F., Lippert, S.C., Laundre, J.A., 2001. Developmental plasticity allows betula nana to dominate tundra subjected to an altered environment. Ecology 82 (1), 18–32.

Christiansen, F.B., 1974. Sufficient conditions for protected polymorphism in a subdivided population. Amer. Nat. 108 (960), 157–166.

Chrzanowski, T.H., Lukomski, N.C., Grover, J.P., 2010. Element stoichiometry of a mixotrophic protist grown under varying resource conditions. J. Eukaryot. Microbiol. 57 (4), 322–327.

Chu, T., Moeller, H.V., Archibald, K.M., 2023. Competition between phytoplankton and mixotrophs leads to metabolic character displacement. Ecol. Model. 481, 110331.
 DeWitt, T.J., Sih, A., Wilson, D.S., 1998. Costs and limits of phenotypic plasticity.

Droop, M.R., 1968. Vitamin b12 and marine ecology. IV. The kinetics of uptake, growth and inhibition in monochrysis lutheri, J. Mar. Biol. Assoc. UK 48 (3), 689–733.

Trends Ecol. Evol. 13 (2), 77-81.

Edwards, K.F., 2019. Mixotrophy in nanoflagellates across environmental gradients in the ocean. Proc. Natl. Acad. Sci. 116 (13), 6211–6220.

Eloranta, A.P., Siwertsson, A., Knudsen, R., Amundsen, P., 2011. Dietary plasticity of arctic charr (salvelinus alpinus) facilitates coexistence with competitively superior european whitefish (coregonus lavaretus). Ecol. Freshw. Fish 20 (4), 558–568.

Eppley, R.W., 1972. Temperature and phytoplankton growth in the sea. Fish. Bull. 70 (4), 1063–1085.

- Field, C.B., Behrenfeld, M.J., Randerson, J.T., Falkowski, P., 1998. Primary production of the biosphere: integrating terrestrial and oceanic components. Science 281 (5374), 237–240.
- Fischer, R., Giebel, H., Hillebrand, H., Ptacnik, R., 2017. Importance of mixotrophic bacteriyory can be predicted by light and loss rates. Oikos 126 (5), 713–722.
- Flynn, K.J., Mitra, A., 2009. Building the perfect beast: modelling mixotrophic plankton. J. Plankton Res. 31 (9), 965–992.
- Flynn, K.J., Stoecker, D.K., Mitra, A., Raven, J.A., Glibert, P.M., Hansen, P.J., Granéli, E., Burkholder, J.M., 2013. Misuse of the phytoplankton–zooplankton dichotomy: the need to assign organisms as mixotrophs within plankton functional types. J. Plankton Res. 35 (1), 3–11.
- Freilich, M., Mignot, A., Flierl, G., Ferrari, R., 2021. Grazing behavior and winter phytoplankton accumulation. Biogeosciences 18 (20), 5595–5607.
- Fulton, E.A., Smith, A., Johnson, C.R., 2003. Effect of complexity on marine ecosystem models. Mar. Ecol. Prog. Ser. 253, 1–16.
- Gonzalez, L.M., Proulx, S.R., Moeller, H.V., 2022. Modeling the metabolic evolution of mixotrophic phytoplankton in response to rising ocean surface temperatures. BMC Ecol. Evol. 22 (1), 1–13.
- Hartmann, M., Grob, C., Tarran, G.A., Martin, A.P., Burkill, P.H., Scanlan, D.J., Zubkov, M.V., 2012. Mixotrophic basis of atlantic oligotrophic ecosystems. Proc. Natl. Acad. Sci. 109 (15), 5756–5760.
- Havskum, H., Hansen, A.S., 1997. Importance of pigmented and colourless nano-sized protists as grazers on nanoplankton in a phosphate-depleted Norwegian Fjord and in enclosures. Aquat. Microb. Ecol. 12 (2), 139–151.
- Iwasa, Y., Andreasen, V., Levin, S., 1987. Aggregation in model ecosystems. I. Perfect aggregation. Ecol. Model. 37 (3-4), 287-302.
- Jones, H., 1997. A classification of mixotrophic protists based on their behaviour. Freshw. Biol. 37 (1), 35–43.
- Kaplan, R.H., Cooper, W.S., 1984. The evolution of developmental plasticity in reproductive characteristics: an application of the adaptive coin-flipping principle. Amer. Nat. 123 (3), 393–410.
- Klausmeier, C.A., Litchman, E., Daufresne, T., Levin, S.A., 2004a. Optimal nitrogen-to-phosphorus stoichiometry of phytoplankton. Nature 429 (6988), 171–174.
- Klausmeier, C.A., Litchman, E., Levin, S.A., 2004b. Phytoplankton growth and stoichiometry under multiple nutrient limitation. Limnol. Oceanogr. 49 (4part2), 1463–1470.
- Leles, S.G., Mitra, A., Flynn, K.J., Stoecker, D.K., Hansen, P.J., Calbet, A., Mc-Manus, G.B., Sanders, R.W., Caron, D.A., Not, F., et al., 2017. Oceanic protists with different forms of acquired phototrophy display contrasting biogeographies and abundance. Proc. R. Soc. B: Biol. Sci. 284 (1860), 20170664.
- Lepik, M., Liira, J., Zobel, K., 2005. High shoot plasticity favours plant coexistence in herbaceous vegetation. Oecologia 145, 465–474.
- Levins, R., 1962. Theory of fitness in a heterogeneous environment. I. The fitness set and adaptive function. Amer. Nat. 96 (891), 361–373.
- Levins, R., 1968. Evolution in Changing Environments: Some Theoretical Explorations. Princeton University Press.
- Li, D.K., Stoecker, A., Coats, D.W., 2000. Spatial and temporal aspects of gyrodinium galatheanum in chesapeake bay: distribution and mixotrophy. J. Plankton Res. 22 (11), 2105–2124.
- Li, T., Yang, F., Xu, J., Wu, H., Mo, J., Dai, L., Xiang, W., 2020. Evaluating differences in growth, photosynthetic efficiency, and transcriptome of asterarcys sp. scs-1881 under autotrophic, mixotrophic, and heterotrophic culturing conditions. Algal Res. 45, 101753.
- Lie, A.A., Liu, Z., Terrado, R., Tatters, A.O., Heidelberg, K.B., Caron, D.A., 2018. A tale of two mixotrophic chrysophytes: Insights into the metabolisms of two ochromonas species (chrysophyceae) through a comparison of gene expression. PLoS One 13 (2), e0102430
- Lipowsky, A., Roscher, C., Schumacher, J., Michalski, S.G., Gubsch, M., Buchmann, N., Schulze, E., Schmid, B., 2015. Plasticity of functional traits of forb species in response to biodiversity. Perspect. Plant Ecol. Evol. Syst. 17 (1), 66–77.
- Litchman, E., 2007. Resource competition and the ecological success of phytoplankton. In: Evolution of Primary Producers in the Sea. Elsevier, pp. 351–375.
- Litchman, E., Klausmeier, C.A., Schofield, O.M., Falkowski, P.G., 2007. The role of functional traits and trade-offs in structuring phytoplankton communities: scaling from cellular to ecosystem level. Ecol. Lett. 10 (12), 1170–1181.
- López-Urrutia, A., San Martin, E., Harris, R.P., Irigoien, X., 2006. Scaling the metabolic balance of the oceans. Proc. Natl. Acad. Sci. 103, 8739–8744, URL www.pnas. orgcgidoi10.1073pnas.0601137103.
- Michaelis, L., Menten, M.L., 1913. Die kinetik der invertinwirkung. Biochem. Z. 49 (333–369), 352.
- Milberg, P., Karlsson, J., Wessman, L., Karlsson, L.M., 2014. Do differences in plasticity during early growth lead to differing success in competition? a test using four co-occurring annual p apaver. Plant Species Biol. 29 (1), 92–100.

- Millette, N.C., da Costa, M., Mora, J.W., Gast, R.J., 2021. Temporal and spatial variability of phytoplankton and mixotrophs in a temperate estuary. Mar. Ecol. Prog. Ser. 677, 17–31.
- Miner, B.G., Sultan, S.E., Morgan, S.G., Padilla, D.K., Relyea, R.A., 2005. Ecological consequences of phenotypic plasticity. Trends Ecol. Evol. 20 (12), 685–692.
- Mitra, A., Flynn, K.J., Burkholder, J.M., Berge, T., Calbet, A., Raven, J.A., Granéli, E., Glibert, P.M., Hansen, P.J., Stoecker, D.K., et al., 2013. The role of mixotrophic protists in the biological carbon pump. Biogeosci. Discuss. 10 (8).
- Mitra, A., Flynn, K.J., Tillmann, U., Raven, J.A., Caron, D., Stoecker, D.K., Not, F., Hansen, P.J., Hallegraeff, G., Sanders, R., et al., 2016. Defining planktonic protist functional groups on mechanisms for energy and nutrient acquisition: incorporation of diverse mixotrophic strategies. Protist 167 (2), 106–120.
- Molina-Montenegro, M.A., Penuelas, J., Munné-Bosch, S., Sardans, J., 2012. Higher plasticity in ecophysiological traits enhances the performance and invasion success of taraxacum officinale (dandelion) in alpine environments. Biol. Invasions 14, 21–33.
- Moorthi, S.D., Ptacnik, R., Sanders, R.W., Fischer, R., Busch, M., Hillebrand, H., 2017.

  The functional role of planktonic mixotrophs in altering seston stoichiometry.

  Aquat. Microb. Ecol. 79 (3), 235–245.
- Murren, C.J., Auld, J.R., Callahan, H., Ghalambor, C.K., Handelsman, C.A., Heskel, M.A., Kingsolver, J.G., Maclean, H.J., Masel, J., Maughan, H., et al., 2015. Constraints on the evolution of phenotypic plasticity: limits and costs of phenotype and plasticity. Heredity 115 (4), 293–301.
- Nilsson, N., 1967. Interactive segregation between fish species. In: The Biological Basis of Freshwater Fish Production. pp. 295–313.
- Nowicki, M., DeVries, T., Siegel, D.A., 2022. Quantifying the carbon export and sequestration pathways of the ocean's biological carbon pump. Glob. Biogeochem. Cycles 36 (3), e2021GB007083.
- Pahl-Wostl, C., 1997. Dynamic structure of a food web model: comparison with a food chain model. Ecol. Model. 100 (1–3), 103–123.
- Pérez, M.T., Dolan, J.R., Fukai, E., 1997. Planktonic oligotrich ciliates in the nw mediterranean: growth rates and consumption by copepods. Mar. Ecol. Prog. Ser. 155, 89–101.
- Rose, J.M., Caron, D.A., 2007. Does low temperature constrain the growth rates of heterotrophic protists? evidence and implications for algal blooms in cold waters. Limnol. Oceanogr. 52, 886–895.
- Schenone, L., Balseiro, E., Modenutti, B., 2022. Light dependence in the phototrophyphagotrophy balance of constitutive and non-constitutive mixotrophic protists. Oecologia 200 (3-4), 295–306.
- Seebacher, F., White, C.R., Franklin, C.E., 2015. Physiological plasticity increases resilience of ectothermic animals to climate change. Nature Clim. Change 5 (1), 61 66
- Seger, J., Brockmann, H.J., Harvey, P.H., Partridge, L., 1987. Oxford surveys in evolutionary biology. In: Oxford Surveys in Evolutionary Biology. Vol. 4, pp. 182–211.
- Selosse, M., Charpin, M., Not, F., 2017. Mixotrophy everywhere on land and in water: the grand écart hypothesis. Ecol. Lett. 20 (2), 246–263.
- Stoecker, D.K., 1998. Conceptual models of mixotrophy in planktonic protists and some ecological and evolutionary implications. Eur. J. Protistol. 34 (3), 281–290.
- Stoecker, D.K., H, P.J., Caron, D.A., Mitra, A., 2017. Mixotrophy in the marine plankton. Annu. Rev. Mar. Sci. 9, 311–335.
- Turcotte, M.M., Levine, J.M., 2016. Phenotypic plasticity and species coexistence. Trends Ecol. Evol. 31 (10), 803–813.
- Van Buskirk, J., Steiner, U.K., 2009. The fitness costs of developmental canalization and plasticity. J. Evol. Biol. 22 (4), 852-860.
- Walsh, J.B., 1984. Hard lessons for soft selection. Amer. Nat. 124 (4), 518-526.
- Ward, B.A., Dutkiewicz, S., Barton, A.D., Follows, M.J., 2011. Biophysical aspects of resource acquisition and competition in algal mixotrophs. Amer. Nat. 178 (1), 98–112.
- Ward, B.A., Follows, M.J., 2016. Marine mixotrophy increases trophic transfer efficiency, mean organism size, and vertical carbon flux. Proc. Natl. Acad. Sci. 113 (11), 2958–2963.
- Warner, R.R., Chesson, P.L., 1985. Coexistence mediated by recruitment fluctuations: A field guide to the storage effect. Amer. Nat. 125 (6), 769–787.
- Wilken, S., Choi, C.J., Worden, A.Z., 2020. Contrasting mixotrophic lifestyles reveal different ecological niches in two closely related marine protists. J. Phycol. 56 (1), 52–67.
- Yang, C., Hua, Q., Shimizu, K., 2000. Energetics and carbon metabolism during growth of microalgal cells under photoautotrophic, mixotrophic and cyclic light-autotrophic/dark-heterotrophic conditions. Biochem. Eng. J. 6 (2), 87–102.
- Zubkov, M.V., Tarran, G.A., 2008. High bacterivory by the smallest phytoplankton in the north atlantic ocean. Nature 455 (7210), 224–226.